hope that these results will stimulate further microwave spectral studies on acetamide.

Calculations

The calculations were carried out with a development version of GAUSSIAN 91 system of programs.[6] Standard basis sets were used.[5] The analysis of the wave functions was carried out with the PROAIM programs.[14] The bond orders were calculated using BONDER.[13]

Acknowledgment. This research was supported by a grant from the National Institutes of Health.

Registry No. $AcNH_2$, 60-35-5; $AcNH_2 \cdot H_2O$, 137647-89-3.

(14) Biegler-Konig, F. W.; Bader, R. F. W.; Tang, T.-H. *J. Comput. Chem.* **1982**, *3*, 317.

Analysis of the Effect of Electron Correlation on Charge Density Distributions

Kenneth B. Wiberg,* Christopher M. Hadad, Teresa J. LePage, Curt M. Breneman,

Department of Chemistry, Yale University, New Haven, Connecticut 06511

and Michael J. Frisch*

Lorentzian, Inc., North Haven, Connecticut 06473 *(Received: September 20, 1991)*

An analysis of charge density distributions is presented for some simple systems with several bond types. Correlated densities from Møller–Plesset perturbation theory to second-order (MP2), configuration interaction with single and double excitations (CISD) and quadratic CI (QCI) were obtained from the Z density, an effective density matrix which represents the response of the correlated system to any one-electron perturbation. These densities are compared with densities derived by integrating the CI wave function and with SCF densities. The difference between the Z density and the unrelaxed density is usually small, but it is significant in some instances. The change in density is exaggerated by MP2 compared to CISD or QCI. The unusual cases of CO (in which different correlation methods give substantially different dipoles) and malonaldehyde enol (in which the hydrogen bond geometry changes significantly on inclusion of correlation) are examined in detail.

Introduction

Charge density distributions have been widely used in studies of molecular structure and bonding. A number of factors are known to limit the quality of theoretically determined charge densities as calculated from Hartree–Fock wave functions.[1] Principal among these are the effects of finite basis sets, relativistic effects, vibrational motion, and electron correlation. The present work examines the last of these in light of new developments in density representations of correlated wave functions.

The effect of electron correlation on the charge density distribution in many stable molecules should represent a small correction compared to both basis set variations and the accuracy of experimental observations. It has been shown to be important, however, in determining the dipole orientation of CO. The inclusion of electron correlation is necessary for the description of systems poorly described by a single determinant. Correlated electron density distributions have previously been obtained by evaluating the density corrected to second order in perturbation theory or integrating the CI wave function[2,3] at representative points in space about the molecules in question.[3-5] Incomplete correlation methods such as CISD do not satisfy the Hellmann–Feynman theorem. As a result, one-electron properties such as the dipole moment calculated from expectation values give values different from the same properties calculated as the energy derivatives. Derivative methods have been deemed superior since they represent the wave function response to a perturbation and is thus more closely tied to experimental observables.[6,7] Derivative methods can also be used to obtain higher order properties, such as polarizabilities, while the expectation value can not.

The Z-vector method originally given by Handy and Schaefer[8] has proven very useful in the evaluation of post-Hartree–Fock derivatives. This method has also simplified the calculation of one-electron properties in incomplete CI wave functions that do not satisfy the Hellmann–Feynman theorem. The Z vector is obtained from CI gradient calculations[9] and acts as a relaxation correction to the one-particle density matrix. The sum of the Z vector and the one-particle density matrix gives an effective correlated density matrix which has been used to calculate one-electron properties, such as the dipole moment, and which includes the energy derivative part of the Hellmann–Feynman inequality.[10,11] Since this sum (which we will call the relaxed density) is a derivative-based density matrix, it is more appropriate for the study of electron density distribution than the CI one-particle density. The use of the relaxed density as a true density matrix has been noted previously for the special cases of CI wave functions[8] and MCSCF plus CI wave functions[9] and can be applied to all correlation methods,[12] including second order[7] and higher order[9] Møller–Plesset gradient calculations. As a derivative method, it is superior to the alternative approach of calculating the density correct to second order.[13] For those models in which no wave function corresponds to the energy (such as perturbation theory) or for which the wave function is not easily manipulated

(1) Breitenstein, M.; Dannöhl, H.; Meyer, H. In *Electron Distributions and the Chemical Bond*; Coppens, P., Hall, M. B., Eds.; Plenum Press: New York, 1982; pp 255-281.
(2) See, for example: Shavitt, I. In *Methods of Electronic Structure Theory*; Schaefer, H. F., Ed.; Plenum Press: New York, 1977; pp 189-275.
(3) Boyd, R. J.; Wang, L.-C. *J. Comput. Chem.* **1989**, *10*, 367.
(4) Stephens, M. E.; Becker, P. J. *Mol. Phys.* **1983**, *49*, 65-89.
(5) Ritchie, J. P.; King, H. F.; Young, W. S. *J. Chem. Phys.* **1986**, *85*, 5175-5181.
(6) Raghavachari, K.; Pople, J. A. *Int. J. Quantum Chem.* **1981**, *20*, 1067-1071.
(7) Dierckson, G. H. F.; Roos, B. O.; Sadlej, A. J. *Chem. Phys.* **1981**, *59*, 29-39.
(8) Handy, N. C.; Schaefer, H. F. *J. Chem. Phys.* **1984**, *81*, 5031-5034.
(9) Shepard, R. L. In *NATO ASI Ser., Ser. C* **1986**, *166* (Geom. Deriv. Energy Surf. Mol. Prop.), 193-206.
(10) Salter, E. A.; Trucks, G. W.; Fitzgerald, G.; Bartlett, R. J. *Chem. Phys. Lett.* **1987**, *141*, 61-70.
(11) Rendell, A. P. L.; Bacskay, G. B.; Hush, N. S.; Handy, N. C. *J. Chem. Phys.* **1987**, *87*, 5976-5986.
(12) Frisch, M. J.; Pople, J. A. Unpublished work.
(13) Amos, R. D. *Chem. Phys. Lett.* **1980**, *73*, 602-606.

0022-3654/92/2096-671$03.00/0

TABLE I: Energies Calculated Using the MP2/6-31G* Optimized Geometry[a]

	RHF			MP2			CISD		QCI
	6-31G*	6-31G**	6-311++G**	6-31G*	6-31G**	6-311++G**	6-31G**	6-311++G**	6-311++G**
C_2H_6	-79.228 54	-79.238 03	-79.251 84	-79.503 97	-79.553 61	-79.613 30	-79.558 75	-79.614 40	-79.649 73
C_2H_4	-78.031 07	-78.038 19	-78.055 59	-78.294 29	-78.327 15	-78.388 08	-78.330 47	-78.386 93	-78.417 47
C_2H_2	-76.815 59	-76.819 69	-76.840 62	-77.076 22	-77.091 43	-77.153 74	-77.085 88	-77.144 01	-77.170 38
CH_2O	-113.836 72	-113.867 22	-113.899 91	-114.174 96	-114.190 99	-114.286 82	-114.179 74	-114.268 63	-114.300 75
CO[b]			-112.768 48			-113.123 36		-113.103 89	-113.130 31
HF	-100.002 29	-100.010 35	-100.051 79	-100.184 16	-100.196 52	-100.305 41		-100.298 04	-100.307 25
H_2O	-76.009 81	-76.022 24	-76.051 86	-76.199 24	-76.222 33	-76.299 28		-76.294 83	-76.305 78
NH_3	-56.183 84	-56.194 90	-56.214 01	-56.357 38	-56.386 84	-56.437 81		-56.441 12	-56.452 07
H_2S	-398.667 11	-398.674 84	-398.702 16	-398.798 70	-398.821 00	-398.970 32		-398.975 45	
PH_3	-342.447 75	-342.454 02	-342.477 97	-342.562 26	-342.590 03	-342.739 09		-342.748 48	
SiH_4	-291.225 05	-291.230 77	-291.253 32	-291.316 85	-291.349 70	-291.498 12		-291.511 37	

[a] In hartrees. [b] The MP2/6-311+G*(6d) optimized geometry was used.

(such as QCI[14] or coupled-cluster[15]), the Z density represents the only consistent approach to examining the correlation effects on electron density. Since the MP2 method is more feasible than CI on large molecular systems (such as conjugated and aromatic organic molecules) in which correlation may play an important role, the ability to obtain densities from MP2 calculations greatly increases the range of systems for which correlated electron densities can be studied.

The difference between the energy derivative and expectation value methods for calculating correlated one-electron properties, principally dipole moments, has been studied in several different systems.[16] The difference in dipole and higher multipole moments is often small in stable molecules, but a large difference was found for the dipole moment of CO calculated with only double excitations in the correlation interaction. The qualitative difference in spatial electron distributions given by the two methods has not previously been examined. In general, it is expected that the difference between the two methods can be large when the correlation contribution to the wave function itself is large. In practice, not enough different cases have been examined in this or any previous study to predict when the two methods differ substantially, and we feel the energy derivative method should be used exclusively since it represents negligible additional calculational effort after the CI calculation.

MP2 relaxed densities have not previously been studied. Due to the known limitations of the MP2 method for the calculation of energies, it is expected that MP2 densities should give poorer descriptions of the electron density distributions than CISD densities. One would anticipate that the QCI densities should be more satisfactory than either of the other methods. The differences between the density distributions found via the three methods will be outlined below. In addition, the effect of basis set on the electron populations derived from the charge densities will be examined.

Methods

Calculations were done using GAUSSIAN 90[17] on a Multiflow Trace 7/200 and 14/300 computers as well as with a Vaxstation GPX. Standard basis sets were used, and the 6D option was used for the d polarization functions. CISD, QCISD (referred to in this report as QCI), and MP2 calculations included all electrons. Hartree–Fock, relaxed, and unrelaxed density matrices were used to generate planes or cubes of charge densities, 80 per side, from which the contour illustrations were generated. The density matrices were converted to natural orbitals that were used in the normal fashion to calculate atomic charge densities and critical point properties.[18]

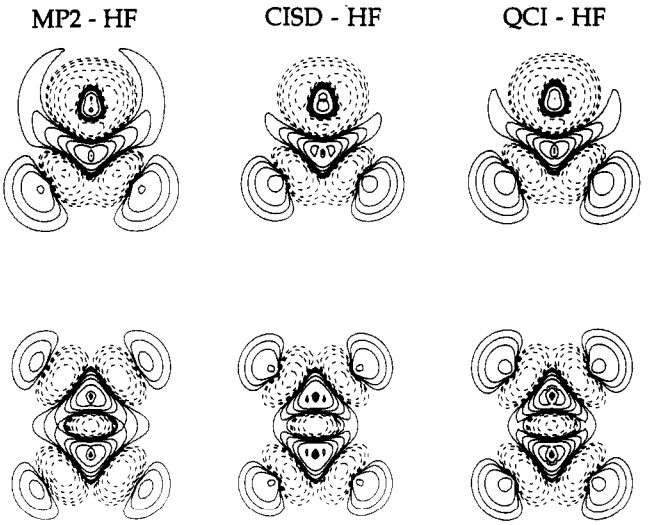

Figure 1. Changes in charge density distributions on going from Hartree–Fock to correlated wave functions. The upper plots are for the molecular plane of formaldehyde (the carbonyl oxygen is up), and the lower plots are for ethylene. The outer contour is 2×10^{-4} e/au^2 and they increase to 4, 8, 20, 40, 80... $\times 10^{-4}$ e/au^2.

Effect of Electron Correlation on Charge Density Distributions

Several simple small molecules with polar, covalent, and multiple bond types were chosen to study the relation between the densities obtained by different methods. The systems studied are given in Table I. The set of simple hydrides was examined to explore the effects of increasing bond polarity, and the C_2 hydrocarbons ethane, ethylene, and acetylene were examined as representatives of covalent bonds. Formaldehyde was used to examine the carbonyl linkage. To have a consistent set of geometries for all of the calculations, we have used those derived via MP2/6-31G* optimizations that are known to be close to the experimental geometries. We wished to minimize basis set size effects, and therefore we have obtained all of the densities using 6-311++G** which is effectively triple ζ for the valence electrons and includes both diffuse and polarization functions on all of the atoms.[19] The energies of the molecules calculated at the different levels of correction for electron correlation are given in Table I.

The effect of electron correlation on ethylene and formaldehyde is shown in Figure 1, which shows the difference in charge density in molecular planes on going from the HF density to each of several correlated relaxed densities. Similar results for formaldehyde have been reported by Boyd and Wang[3] using approximate MP2 and CISD wave functions.[20] As has been previously

(14) Pople, J. A.; Head-Gordon, M.; Raghavachari, K. *J. Chem. Phys.* **1987**, *87*, 5968–5975.
(15) Pople, J. A.; Raghavachari, K.; Schlegel, H. B.; Binkley, J. S. *Int. J. Quantum Chem.* **1978**, *14*, 545–560.
(16) For example, see refs 6 and 7.
(17) GAUSSIAN 90; Frisch, M. J.; Head-Gordon, M.; Trucks, G. W.; Foresman, J. B.; Schlegel, H. B.; Raghavachari, K.; Robb, M. A.; Binkley, J. S.; Gonzalez, C.; Defrees, D. J.; Fox, D. J.; Whiteside, R. A.; Seeger, R.; Melius, C. F.; Baker, J.; Martin, R. L.; Kahn, L. R.; Stewart, J. J. P.; Topiol, S.; Pople, J. A. Gaussian, Inc.: Pittsburgh, PA, 1990.
(18) Biegler-König, F. W.; Bader, R. F. W.; Tang, T.-H. *J. Comput. Chem.* **1982**, *3*, 317. Bader, R. F. W. *Atoms in Molecules. A Quantum Theory*; Oxford University Press: Oxford, 1990.
(19) (a) Clark, T.; Chandrasekhar, J.; Spitznagel, G. W.; Schleyer, P. v. R. *J. Comput. Chem.* **1983**, *4*, 294. (b) Frisch, M. J.; Pople, J. A.; Binkley, J. S. *J. Chem. Phys.* **1984**, *80*, 3265.

TABLE II: Negative Difference Sum from Comparison of Different Correlation Methods[a]

	MP2 - RHF	CISD - RHF	QCI - RHF	MP2/relax[c]	CISD/relax[c]
C_2H_6	−0.118	−0.075	−0.100	−0.031	−0.007
C_2H_4	−0.121	−0.093	−0.119	−0.033	−0.016
CH_2O	−0.161	−0.108	−0.138	−0.046	−0.018
CO[b]	−0.176	−0.110	−0.136	−0.056	−0.013
cis-malonaldehyde	−0.369				
cis-malonaldehyde enol	−0.402				
trans-malonaldehyde enol	−0.370				

[a] In units of electrons. Unless otherwise specified, the generalized density matrices were used. [b] MP2/6-311+G*(6d) geometry was used; all others are the MP2/6-31G* geometry. [c] The difference between the relaxed and unrelaxed density matrices.

TABLE III: Deviation of Bond Path Angles from Geometric Angles[a]

	RHF			MP2			CISD		QCI
	6-31G*	6-31G**	6-311++G**	6-31G*	6-31G**	6-311++G**	6-31G**	6-311++G**	6-311++G**
C_2H_6									
C-C-H	0.94	0.91	0.90	1.15	1.15	1.11	1.00	0.97	0.98
H-C-H	−0.98	−0.95	−0.94	−1.20	−1.20	−1.16	−1.05	−1.01	−1.02
C_2H_4									
C-C-H	−0.87	−1.00	−1.13	−0.42	−0.56	−0.70	−0.71	−0.88	−0.82
H-C-H	1.74	2.00	2.25	0.85	1.12	1.39	1.43	1.77	1.63
CH_2O									
O-C-H	−0.36	−0.51	−0.58	0.26	0.08	0.18	−0.14	−0.16	−0.03
H-C-H	0.72	1.01	1.17	−0.52	−0.15	−0.36	0.27	0.31	0.06
H_2O									
H-O-H	4.39	4.04	3.90	3.39	2.97	3.08		3.53	3.47
NH_3									
H-N-H	3.17	2.97	2.52	2.63	2.38	2.00		2.32	2.28
H_2S									
H-S-H	−3.78	−4.00	−4.16	−3.59	−3.91	−4.04		−4.00	
PH_3									
H-P-H	−3.75	−3.71	−3.75	−3.59	−3.62	−3.64		−3.62	

[a] Units in degrees and using the MP2/6-31G* geometry.

noted,[4] the usual effect of electron correlation on the electron distribution is to deplete electron density from the centers of bonds and increase it in shells around the atomic nuclei and at the periphery of the molecule. The QCI density would be expected to be closest to the true density. Using this as the reference, it can be seen that for formaldehyde, MP2 exaggerates the shift in charge density, and that CISD tends to give too small a shift. With ethylene, the differences were smaller but still significant.

The differences between the three correlated densities were smaller for the plane containing the π-electrons, and the QCI − HF difference for formaldehyde and ethylene is shown in Figure 2. Again, the major effect was to remove charge density from the bonding region.

We were interested in determining how large a shift in charge density occurred for each of the levels of correction for electron correlation. As a measure of this quantity, we integrated separately the positive and negative differences found in differences in cubes of charge density. The values are summarized in Table II. It can be seen that all the correlated methods yield a difference of about 0.1 e with respect to the HF density. The MP2 density provided a slightly larger difference than QCI, whereas CISD tends to give too small a shift in density. This parallels the trends seen in Figure 1. The difference between the unrelaxed and relaxed densities also was of interest. The CISD relaxed density was similar to the unrelaxed density with only about a 0.01 e difference. However, the MP2 relaxed density has a 0.04 e difference from its unrelaxed representation.

Bond Path Angles

The conventional bonds (i.e., lines drawn between nuclear centers) often do not well represent bonding in the molecules. The bond paths (the paths of maximum charge density between bonded nuclei) are frequently curved. This has been explored previously for a number of molecules[21] including many that are examined in this report. Therefore, it was of interest to us to see how basis set size and correction for electron correlation will affect the angles between the bond paths. The differences between the conventional and bond path angles have been calculated and are summarized in Table III.

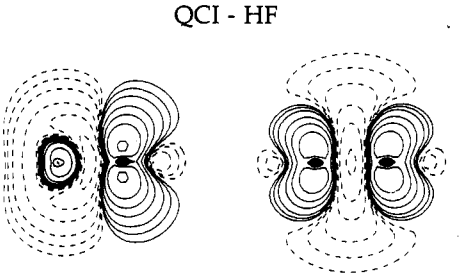

Figure 2. Changes in charge density on going from the Hartree–Fock to QCI densities for the π-electron planes of formaldehyde (left, the carbonyl oxygen is to the left) and for ethylene (right). The contour levels are the same as for Figure 1.

The effect of basis set on the angular deviation was generally fairly small. The magnitude of the difference between the two angles was generally smaller with the inclusion of electron correlation, and again MP2 appeared to exaggerate the deviation, whereas CISD did not give a large enough difference. In general, the conclusions drawn from the RHF densities are consistent with the results obtained using the correlated densities. Thus, for water and ammonia, the bond path angles were smaller than the conventional angles, indicating that the bonds are bent outwards due to H···H nonbonded repulsion. With the longer third-row hydride bonds (S–H and P–H), the H···H repulsion is smaller, and the bond path angles were bent inward, presumably due to lone pair–hydrogen repulsion.

Electron Populations

We were interested in examining the effect of both basis set size and of electron correlation on the electron populations derived

(20) Their MP2 density is that obtained at first order in perturbation theory plus a correction for single excitations only at second order. Their CI density is an approximation to the CI one-particle density obtained by using only two CI iterations rather than converging the CI wave function.

(21) Wiberg, K. B.; Murcko, M. A. *J. Mol. Struct.* **1988**, *169*, 355.

TABLE IV: Percentage of Charge Density (Relative to RHF) at the Bond Critical Point[a]

	MP2			CISD		QCI
	6-31G*	6-31G**	6-311++G**	6-31G**	6-311++G**	6-311++G**
C_2H_6						
C–C	−3.5	−3.4	−4.5	−2.3	−2.9	−3.6
C–H	−1.6	−1.6	−2.3	−1.2	−1.6	−2.3
C_2H_4						
C–C	−2.9	−2.8	−3.2	−2.0	−2.3	−2.8
C–H	−2.0	−2.0	−2.6	−1.6	−1.9	−2.5
C_2H_2						
C–C	−1.6	−1.9	−1.9	−1.4	−1.6	−1.9
C–H	−2.5	−2.5	−2.9	−1.8	−2.0	−2.6
CH_2O						
C–O	−1.6	−1.5	−1.7	−0.9	−1.0	−1.3
C–H	−2.6	−2.8	−3.2	−2.1	−2.4	−3.1
CO[b]						
C–O			−2.1		−1.2	−1.4
HF						
H–F	−0.3	−0.4	−0.8		0.4	0.3
H_2O						
O–H	−1.6	−1.7	−2.0		−0.8	−1.0
NH_3						
N–H	−2.0	−2.1	−2.4		−1.6	−1.9
H_2S						
S–H	−1.7	−1.7	−1.8		−1.5	
PH_3						
P–H	−0.6	−0.7	−0.2		−0.4	
SiH_4						
Si–H	−0.6	−0.7	−0.1		−0.2	

[a] Using the MP2/6-31G* optimized geometry. [b] MP2/6-311+G*(6d) geometry was used.

from Bader's theory of atoms in molecules.[22] Here, the bond critical points, the points of minimum charge density along bonds, are first located. Then paths of most rapid decrease in charge density in directions normal to the bond are located, and the set of such paths determines a surface which separates a given pair of atoms. The set of surfaces will separate a molecule into a unique set of atomic domains. Integration of the charge density within a domain gives the electron population for the atom.

An effect of electron correlation on the charge density at the bond critical point was noted, and the percent changes in ρ from the RHF values at the bond critical points for a variety of basis sets are summarized in Table IV. The effect of correlation is to reduce ρ at the critical point, and the largest change was 4%. This again affirms the earlier pictorial view that charge is depleted in the bonding regions for correlated densities as compared to RHF.

The effect of basis set size on the calculated electron populations was determined for the HF, MP2, CISD, and QCI levels of theory using the 6-31G*, 6-31G**, and 6-311++G** basis sets giving the results summarized in Table V. It is known that 6-31G** gives consistently slightly larger electron populations at H than 6-31G*, largely as a result of a small shift in the bond critical point on going to the better balanced basis set.[23] The more flexible 6-311++G** basis should provide the better representation of the charge density, and here, with the first-row hydrides, the populations are intermediate between those found with the smaller basis sets.

For both compounds having carbonyl groups, the more flexible basis sets was found necessary for a better description of the charge distribution about oxygen, and there was no clear trend for the three basis sets. Water, on the other hand, follows the trend for the other first-row hydrides.

The second-row hydrides gave larger changes in the atomic charges with changes in basis set. The more flexible basis sets lead to a positive charge at S in H_2S for both RHF and the correlated levels. Phosphorus behaves similarly, but silicon behaves more like the first-row hydrides.

It was of interest to see the difference between the use of the unrelaxed and the relaxed density matrices, and this was studied using the 6-311++G** basis set. The results are included in Table V (unrelaxed values are given in parentheses). Although the differences in population calculated using the two density matrices were significant, they were not large; however, the differences are smaller for the CISD representations as compared to the MP2 representations.

The changes in populations are at least in part a result of changes in atomic volumes which result from small shifts in the positions of the surfaces which separate pairs of bonded atoms. The volumes calculated at the 0.001 e/au^3 contour level are summarized in Table VI. It can be seen that the changes in volume generally parallel the changes in population. The total molecular volume defined by the sum of the atomic volumes remains, however, essentially constant and independent of basis set or correction for electron correlation.

The depletion of charge density from the centers of bonds on the addition of correlation is observed in most of the covalent and polar bonds in this series. Thus, correlation should have a smaller effect on dipole moments and atomic charges than might be expected from the extent of charge motion away from the centers of bonds since the charge reorganization happens around each atom and can result in only a small net change in polarization of the molecule. The dipole moments as a function of theoretical level of the molecules in this study are given in Table VII. The calculated dipole moments are significantly closer to the experimental values at all levels of electron correlation, but they are still overestimated at all levels. The largest deviation, as compared to RHF, is noted for formaldehyde, and this molecule also corresponds to one of the largest charge reorganizations examined in this study. The Hartree–Fock trends are still evident with the inclusion of correlation.

Results for CO

The magnitude and direction of the dipole of CO have been the subject of much study. Experimental evidence shows that the carbon of CO is at the negative end of the dipole and oxygen is at the positive end.[24] This result is not reproduced in the Har-

(22) Bader, R. F. W. *Atoms in Molecules: A Quantum Theory*; Oxford University Press: Oxford, 1990.

(23) Wiberg, K. B.; Wendoloski, J. J. *Proc. Natl. Acad. Sci. U.S.A.* **1981**, *78*, 6561.

(24) Rosenblum, B.; Nethercot, A. H., Jr.; Townes, C. H. *Phys. Rev.* **1958**, *109*, 400.

TABLE V: Calculated Electron Populations[a]

	RHF			MP2			CISD		QCI
	6-31G*	6-31G**	6-311++G**	6-31G*	6-31G**	6-311++G**	6-31G**	6-311++G**	6-311++G**
C_2H_6									
C	0.065	0.229	0.156	−0.055	0.113	0.029 (0.033)	0.161	0.084 (0.075)	0.069
H	−0.021	−0.074	−0.050	0.019	−0.037	−0.008 (−0.009)	−0.052	−0.026 (−0.023)	−0.021
C_2H_4									
C	−0.052	0.062	−0.002	−0.109	0.011	−0.051 (−0.071)	0.038	−0.023 (−0.037)	−0.026
H	0.026	−0.031	0.001	0.054	−0.005	0.026 (0.035)	−0.019	0.012 (0.019)	0.013
C_2H_2									
C	*b*	*b*	−0.175	−0.195	−0.128	−0.166 (−0.191)	−0.121	−0.159 (−0.169)	−0.157
H	0.190	0.135	0.174	0.191	0.128	0.165 (0.188)	0.120	0.158 (0.168)	0.153
CH_2O									
O	−1.258	−1.259	−1.207	−1.091	−1.089	−1.022 (−1.007)	−1.135	−1.078 (−1.078)	−1.046
C	1.178	1.282	1.168	0.992	1.103	0.976 (0.935)	1.155	1.041 (1.026)	1.010
H	0.040	−0.011	0.020	0.049	−0.007	0.023 (0.036)	−0.010	0.019 (0.026)	0.018
CO[c]									
O			−1.312			−1.094 (−1.079)		−1.176 (−1.166)	−1.141
C			1.312			1.094 (1.079)		1.176 (1.166)	1.141
HF									
F	−0.717	−0.747	−0.744	−0.690	−0.708	−0.706 (−0.699)		0.701 (−0.706)	0.696
H_2O									
O	−1.165	−1.217	−1.194	−1.129	−1.155	−1.126 (−1.117)		−1.109 (−1.113)	−1.098
H	0.582	0.608	0.597	0.564	0.577	0.563 (0.558)		0.554 (0.556)	0.549
NH_3									
N	−1.092	−1.091	−1.059	−1.095	−1.057	−1.036 (−1.035)		−0.998 (−1.011)	−0.989
H	0.364	0.364	0.353	0.365	0.352	0.345 (0.345)		0.333 (0.337)	0.330
H_2S									
S	−0.039	0.284	0.153[d]	−0.082	0.187	0.143 (0.151)[e]		0.199 (0.174)	
H	0.020	−0.142	−0.077	0.041	−0.093	−0.072 (−0.076)		−0.100 (−0.087)	
PH_3									
P	1.629	1.813	1.853	1.437	1.674	1.677 (1.708)		1.707 (1.707)	
H	−0.543	−0.605	−0.619	−0.478	−0.559	−0.560 (−0.570)		−0.570 (−0.570)	
SiH_4									
Si	2.910	2.972	2.964	2.780	2.873	2.833 (2.858)		2.846 (2.851)	
H	−0.725	−0.741	−0.739	−0.693	−0.716	−0.706 (−0.713)		−0.710 (−0.711)	

[a] In units of electrons with the MP2/6-31G* geometry. Populations calculated using one-particle correlated densities are given in parentheses. [b] The carbon atom of acetylene is not rigorously defined in Bader's theory of atoms in molecules at the RHF/6-31G* and RHF/6-31G** levels because of a (3,−3) critical point in the center of the C–C bond. This (3,−3) critical point is not present with more flexible basis sets or when electron correlation is added. [c] Using the MP2/6-311+G*(6d) geometry. [d] Using RHF/6-311++G(2d,p) wave functions. The RHF/6-311++G(d,p) wave functions gave anomalous results. [e] The MP2/6-311++G(2d,p) Z density gave 0.069 at S and −0.034 at H.

TABLE VI: Volume of Atomic Basins at 0.001 e/au^3 Contour Level[a]

	RHF			MP2			CISD		QCI
	6-31G*	6-31G**	6-311++G**	6-31G*	6-31G**	6-311++G**	6-31G**	6-311++G**	6-311++G**
C_2H_6									
C	5.926	5.764	5.837	6.045	5.878	5.962	5.831	5.908	5.923
H	0.999	1.052	1.026	0.959	1.014	0.983	1.029	1.002	0.997
T	17.846	17.840	17.830	17.844	17.816	17.822	17.836	17.828	17.828
C_2H_4									
C	6.028	5.916	5.971	6.084	5.966	6.020	5.940	5.992	5.996
H	0.952	1.008	0.976	0.924	0.983	0.950	0.996	0.965	0.963
T	15.864	15.898	15.886	15.864	15.864	15.840	15.864	15.844	15.844
C_2H_2									
C	*b*	*b*	6.117	6.154	6.088	6.110	6.080	6.103	6.103
H	0.791	0.844	0.806	0.788	0.850	0.814	0.859	0.822	0.826
T			13.846			13.848		13.850	13.858
CH_2O									
O	9.222	9.223	9.159	9.055	9.054	8.970	9.099	9.028	8.994
C	4.806	4.703	4.815	4.991	4.881	5.005	4.829	4.941	4.972
H	0.936	0.986	0.956	0.925	0.980	0.950	0.984	0.956	0.956
T	15.900	15.898	15.886	15.896	15.895	15.875	15.896	15.881	15.878
CO[c]									
O			9.264			9.047		9.129	9.095
C			4.636			4.847		4.770	4.805
T			13.900			13.894		13.899	13.900

[a] In units of (atomic units)^3 using the MP2/6-31G* optimized geometry. [b] These atoms are not rigorously defined using the theory of atoms in molecules at RHF/6-31G* and RHF/6-31G** due to the presence of a (3,−3) critical point at the center of the C–C bond. [c] Using the MP2/6-311+G*(6d) optimized geometry.

tree–Fock limit. The dipole moment at the CID and CISD levels from expectation values ($\langle R \rangle$) and from derivative methods have been previously calculated.[5,6] The CI calculation using singles and doubles gives similar values for the dipole moment using either expectation value or derivative methods, and the sign agrees with experiment. With doubles only, the expectation value gives a sign contrary to experiment, while the derivative method gives the experimentally observed sign. The difference between CID and CISD value of $\langle R \rangle$ has been attributed to "better description of density on inclusion of single excitations".[25]

TABLE VII: Dipole Moment Calculated at Different Theoretical Levels (6-311++G)[a]**

compound	RHF	MP2 unrelaxed	MP2 relaxed	CISD unrelaxed	CISD relaxed	QCI relaxed	expt[b]
H_2CO	−3.022	−2.350	−2.414	−2.648	−2.600	−2.488	−2.332
HF	−2.102	−1.972	−1.998	−1.997	−1.997	−1.982	−1.826
H_2O	−2.259	−2.169	−2.185	−2.182	−2.174	−2.160	−1.855
NH_3	−1.835	−1.792	−1.786	−1.792	−1.779	−1.767	−1.471
H_2S	−1.372	−1.334	−1.323	−1.308	−1.271		−0.973
PH_3	−0.803	−0.804	−0.786	−0.786	−0.727		−0.574

[a] In units of debye. [b] Demaison, J.; Dubrulle, A.; Hüttner, W.; Tiemann, E. *Landolt Bornstein, New Series, II(14a)*, Springer-Verlag: Berlin, 1982.

TABLE VIII: Dipole Moment for Carbon Monoxide at Various Levels of Electron Correlation[a]

geom	C–O, Å	RHF	MP2 unrelaxed	MP2 relaxed	CISD unrelaxed	CISD relaxed	QCI relaxed	expt[b]
RHF	1.104	−0.184	0.479	0.370	0.158	0.123	0.185	
CISD	1.123	−0.277	0.447	0.325	0.090	0.053	0.123	
expt[c]	1.128	−0.305	0.438	0.312	0.070	0.032	0.104	0.110
MP2	1.138	−0.358	0.421	0.287	0.031	−0.007	0.069	

[a] Using the 6-311+G*(6d) basis set at the indicated geometry. [b] Meerts, W. L.; DeLeeuw, F. H.; Dymanus, A. *Chem. Phys.* **1977**, *22*, 319. [c] Mantz, A. W.; Watson, J. K. G.; Rao, K. N.; Albritton, D. L.; Schmeltekopf, A. L.; Zare, R. N. *J. Mol. Spectrosc.* **1971**, *39*, 180.

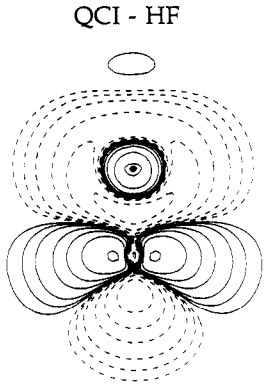

Figure 3. Change in charge density on going from the Hartree–Fock to QCI densities for carbon monoxide. The oxygen is up, and the contour levels are as in Figure 1.

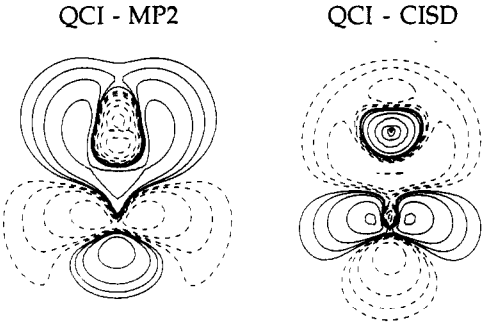

Figure 4. Changes in charge density on going from MP2 or CISD densities to QCI for carbon monoxide.

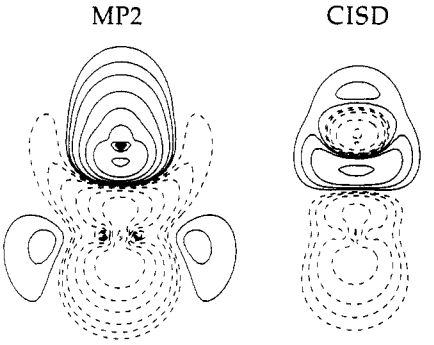

Figure 5. Effect on charge densities for carbon monoxide on going from the one-particle to generalized density matrices for MP2 and CISD wave functions. Solid contours indicate a larger charge density for the generalized density matrix.

Some representative values of the dipole moment calculated as $\langle R \rangle$ and as $\partial\epsilon/\partial E$ (from the relaxed density) for the different levels of theory are listed in Table VIII. These values have been determined using the 6-311++G** basis set. A considerable difference is found between the dipole moments calculated with and without relaxation. Since this discrepancy is an example of a substantial difference between the expectation value and the derivative methods of representing electron distribution, as well as a case in which electron correlation is required to reproduce a qualitative property of the electron distribution, an examination of the electron distribution found with the various methods should be illuminating. We will examine the effect on the electron distribution of correlation, which switches the sign of the dipole, and the effect of relaxation from the expectation value $\langle R \rangle$ to the derivative μ.

The change in charge density on the addition of correlation (QCI) to CO (Figure 3) is somewhat similar to that seen in the C=O bond of formaldehyde. The p orbitals are polarized so that charge is transferred to the carbon π orbitals at the expense of the oxygen π orbitals. Electron density is in turn depleted in the σ orbital at the outside end of the carbon and increased in the oxygen σ orbitals. The resulting change in dipole orientation is the residual of large shifts in electron density that are mostly counterbalanced. The MP2 and CISD relaxed results are qualitatively similar, although again the MP2 differences are more extreme. The difference between the QCI density and those calculated using MP2 and CISD are shown in Figure 4. It can be seen that the QCI density is again intermediate between MP2 and CISD.

The difference between the CISD($\partial\epsilon/\partial E$) and CISD($\langle R \rangle$) densities is very small, but as in the case of H_2CO, the CISD-($\partial\epsilon/\partial E$) puts more electrons on the oxygen (Figure 5). This small difference gives a significant change in dipole moment since the charge shifts all contribute to it instead of canceling. The difference between the MP2($\partial\epsilon/\partial E$) and the density corrected to second order is large and similar to the difference between the correlated and uncorrelated electron densities. In this case the MP2($\partial\epsilon/\partial E$) density description is clearly superior to the density correct to second order in perturbation theory.

The QCI procedure provides the best agreement with the observed dipole moment of CO. The remarkably good agreement supports our assumption that the QCI density provides a good approximation to the true density.

(25) Szabo, A.; Ostlund, N. S. *Modern Quantum Chemistry: Introduction to Advanced Electronic Structure Theory*; Macmillan: New York, 1982.

TABLE IX: Total Energies[a] and Selected Geometric Parameters[b] for Malonaldehyde

	RHF		MP2	
	6-31G*	6-311++G**	6-31G*	6-311++G**
cis-malonaldehyde (**2**)	-265.621 32	-265.695 92	-266.374 22	-266.622 21
cis-malonaldehyde enol (**1a**)	-265.626 82	-265.706 56	-266.382 95	-266.635 84
trans-malonaldehyde enol (**1b**)	-265.607 19	-265.689 24	-266.360 11	-266.616 51

	cis-dione	*trans*-enol	*cis*-enol		
	MP2/6-31G*	MP2/6-31G*	MP2/6-31G*	expt[c]	MP2/6-31G**[d]
r(C—C)	1.512	1.463	1.441	1.454	1.439
r(C=C)		1.348	1.362	1.348	1.362
r(C=O)	1.219	1.229	1.248	1.234	1.248
r(C—O)		1.352	1.330	1.320	1.328
r(O—Ha)		0.972	1.000	0.969	0.994
r(C—Hb)		1.090	1.087	1.089	1.083
r(C—Hc)	1.101	1.085	1.083	1.091	1.077
r(C—Hd)	1.111	1.110	1.103	1.094	1.098
r(O--O)	2.991	2.809	2.623	2.553	2.589
∠C=C—C	119.1	125.1	120.0	119.4	119.5
∠C—C=O	126.5	125.6	123.7	123.0	123.5
∠C=C—O		123.4	124.9	124.5	124.5
∠C—O—Ha		108.8	105.9	106.3	105.4

[a] In hartrees. [b] Bond distances in angstroms and angles in degrees. [c] Reference 26. [d] Reference 28.

TABLE X: Percentage of Charge Density (MP2 - RHF) at the Bond Critical Point for Malonaldehyde[a]

bond	*cis*-dione	*trans*-enol	*cis*-enol
C—C	-5.0	-4.7	-4.3
C=C		-3.0	-3.0
C=O	-1.9	-2.3	-2.8
C—O		-1.8	-2.5
O—Ha		-2.1	-0.7
C—Hb	-3.5	-3.6	-3.6
C—Hc	-3.1	-2.6	-2.4
C—Hd		-3.7	-3.7

[a] Using the 6-311++G**(6d) basis set with the MP2/6-31G* geometry.

Malonaldehyde

The cyclic conformation of malonaldehyde enol (**1a**) is the simplest example of an intramolecular hydrogen bond and has an interesting six-membered ring arrangement. The geometry of **1a** has been well studied experimentally. An extensive series of 28 isotopically substituted malonaldehydes have been studied by Wilson and co-workers in order to assign the infrared spectrum and determine structural parameters from microwave spectra.[26] From this work the H–O and O–O distances as well as all bond lengths and angles are known with good accuracy. The barrier to proton transfer has been estimated to be 4–5.2 kcal/mol.[27]

Ab initio calculations of the geometry offered an interesting case for comparison of experiment with theory. The STO-3G structure is in reasonable agreement with the experimental findings, yet larger bases in the single-configuration limit (DZ and DZP, etc.) give geometries in poorer agreement with the experimental geometry.[28] In particular, the O–H and O–O distances were calculated to be too large. The vibrational frequencies obtained at the Hartree–Fock level suggested an alternative assignment to that proposed by Wilson,[29] but the calculated O–H stretch was too high (by 30%), the C=O stretch was too high (by 17%). The proton-transfer barrier, at 10–20 kcal/mol depending on basis level, was also high compared to experiment.

The O—H and O—O distances found at the MP2/6-31G** level compared well with the experimental geometry.[26] The proton-transfer barrier was also lowered greatly on the addition of correlation. The MP2/6-31G** vibrational frequencies and intensities agree well with assignment II of Wilson, and the O—H and C=O frequencies are in better agreement with experiment.[30] Thus correlation reduces O—O repulsion and reduces the barrier to proton transfer. An examination of the density difference maps of **1a** may highlight the important interactions contributing to the observed energy differences. To this end, we have considered three forms of malonaldehyde: the *cis*-dione (**2**) and the *cis*-(**1a**) and *trans*-enol (**1b**) forms.

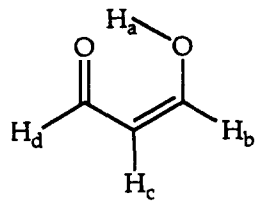

1a

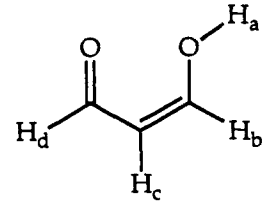

1b

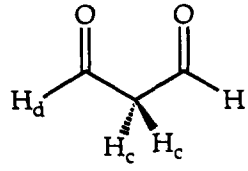

2

Quantitatively, **1a** shows the largest difference in the total charge distribution for all of the molecules considered in this study. The total difference sum amounts to 0.4 e for MP2–RHF, and the charge shift is only slightly smaller (0.37 e) for **1b** and **2** (Table II). Interestingly, the other large charge shifts are those for the carbonyl-containing compounds, and it is for these compounds that the effect of electron correlation is most important for accurate geometries and other properties. In addition, the charge shift for **2** is almost twice that for formaldehyde and may be an additive effect for carbonyl groups. The *cis*-enol (**1a**) shows a slightly larger correlation effect than either **1b** or **2**.

Density difference maps obtained by subtracting the RHF density from the MP2 density using the 6-311++G** basis are presented in Figure 6 for **2** and both **1a** and **1b**. Within the molecular plane, it is readily apparent that electron correlation decreases charge density within the bonding regions between nuclei (as seen above) and on the nuclei themselves, but also increases it in the diffuse regions around atoms. This presumably will reduce

(26) Baughcum, S. L.; Duerst, R. W.; Rowe, W. F.; Smith, Z.; Wilson, E. B. *J. Am. Chem. Soc.* **1981**, *103*, 6296.
(27) Baughcum, S. L.; Smith, Z.; Wilson, E. B.; Duerst, R. W. *J. Am. Chem. Soc.* **1984**, *106*, 2260.
(28) Frisch, M. J.; Scheiner, A. C.; Schaefer, H. F., III; Binkley, J. S. *J. Chem. Phys.* **1985**, *82*, 4194.
(29) Smith, Z.; Wilson, E. B.; Duerst, R. W. *Spectrochim. Acta* **1983**, *39A*, 1117.
(30) Binkley, J. S.; Frisch, M. J.; Schaefer, H. F. *Chem. Phys. Lett.* **1986**, *126*, 1.

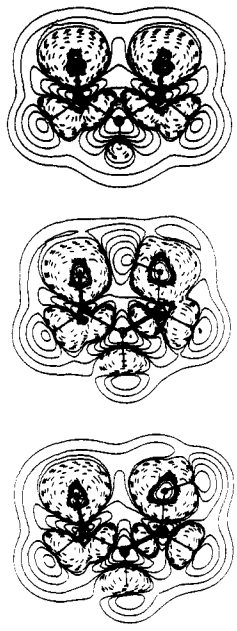

Figure 6. Effect on the σ-charge densities for malonaldehyde and its enols on going from the HF to MP2 densities. The outer contour is 1 $\times 10^{-4}$ e/au^2 and they increase by factors of 2.

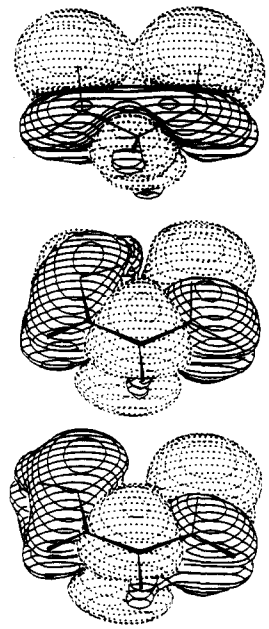

Figure 7. Effect on π-charge densities for malonaldehyde and its enols on going from the HF to MP2 densities. The contour levels are the same as for Figure 6.

electron–electron repulsions. For both **1a** and **1b**, there is a charge concentration at the MP2 level in the intermediate region between the two oxygens, thus allowing the two oxygen atoms to approach each other more closely. This effect is most pronounced for **1a** as the hydroxyl hydrogen resides within this concentration region. Consequently, the barrier for proton transfer is reduced with the addition of electron correlation over that obtained using Hartree–Fock theory. Using the MP2/6-31G* geometry (Table IX), the distance between the oxygens reflects this stabilization due to the hydroxyl H: **2** (2.991 Å), **1b** (2.809 Å), and **1a** (2.623 Å, expt 2.553–2.576 Å).

In Table X, we have listed the percentage change in the value of ρ at the bond critical point for the malonaldehyde tautomers, and as seen above, there is a loss of charge density in the bonding regions between atoms. The largest change as compared to RHF is 5%.

To probe the cause of this effect, we have analyzed both the σ and the π contributions to the charge density difference. The corresponding difference maps are presented in Figure 7 for **2**, **1a**, and **1b**. Within the π system, there is the general trend to concentrate charge density on the carbons at the expense of the oxygens for each carbonyl group. The C—OH ether linkage, on the other hand, undergoes charge concentration with simultaneous depletion of π density from the C=C bond with the inclusion of electron correlation. Within the σ system (Figure 6), the changes within the molecular plane mirror the overall effect for the total density, and thus, it is the major contributor to the overall charge shift in the molecule. This effect is also evident in the larger magnitude for the density difference sums within the different symmetry spaces for the **1a** (σ, −0.2522; π, −0.2249), **1b** (σ, −0.1947; π, −0.2431), and **2** (σ, −0.1835; π, −0.2514).

Thus, for malonaldehyde, electron correlation removes charge from the bonding regions and increases it in the periphery around and between atoms, and in particular both of the oxygen atoms. This effect reduces electron–electron repulsion and stabilizes **1a** and the corresponding proton transfer.

Conclusions

The relaxed density matrix allows the study of the electron density distribution resulting from the MP2 and CI correlation methods at no significant increase in computational cost over approximations to the density that do not yield analytic derivatives. The electron density differences due to correlation found for reference systems is qualitatively the same for the MP2 and CISD density as has been found previously for unrelaxed CI densities.

TABLE XI: Comparison of Calculated and Experimental Geometries[a]

compound	parameter	MP2/6-31G*	expt[b]
C_2H_6	r(C—C)	1.5249	1.5351 ± 0.0001
	r(C—H)	1.0929	1.0940 ± 0.0002
	∠C—C—H	111.19	111.17 ● 0.01
	∠H—C—H	107.70	
C_2H_4	r(C—C)	1.3349	1.3391 ± 0.0013
	r(C—H)	1.0848	1.0868 ± 0.0013
	∠C—C—H	121.70	121.28 ± 0.10
	∠H—C—H	116.60	117.44 ± 0.10
C_2H_2	r(C—C)	1.2162	1.2024 ± 0.0001
	r(C—H)	1.0659	1.0625 ± 0.0001
CH_2O	r(C—O)	1.2200	1.2078 ± 0.0030
	r(C—H)	1.1039	1.1161 ± 0.0070
	∠O—C—H	122.19	121.75 ± 0.70
	∠H—C—H	115.62	116.50 ± 0.70
CO[c]	r(C—O)	1.1382	1.1282 ± 0.0000
HF	r(H—F)	0.9339	0.9168 ± 0.0000
H_2O	r(O—H)	0.9685	0.9578 ± 0.0000
	∠H—O—H	104.01	104.48 ± 0.00
NH_3	r(N—H)	1.0168	1.0138 ± 0.0010
	∠H—N—H	106.36	107.23 ± 0.20
H_2S	r(S—H)	1.3395	1.3356 ± 0.0030
	∠H—S—H	93.35	92.11 ± 0.30
PH_3	r(P—H)	1.4146	1.4118 ± 0.0005
	∠H—P—H	94.61	93.42 ± 0.06
SiH_4	r(Si—H)	1.4829	1.4819 ± 0.0000

[a] Bond distances in angstroms and bond angles in degrees. [b] Callomon, J. H.; Horota, E.; Iijima, T.; Kuchitsu, K.; Lafferty, W. J. *Landolt-Bornstein*; Springer-Verlag: Berlin, 1987; New Series, Group II(15). Callomon, J. H.; Hirota, E.; Kuchitsu, K.; Lafferty, W. J.; Maki, A. G.; Pote, C. S. *Landolt-Bornstein*; Springer-Verlag: Berlin, 1976; New Series, Group II(7). [c] The MP2/6-311+G*(6d) geometry was calculated in this case.

Compared to the QCI density, MP2 consistently exaggerates the shift in charge density, whereas CISD underestimates the shift. The difference between the unrelaxed and relaxed CISD densities was small in all cases studied compared to the difference between correlated and uncorrelated densities, but considerably larger differences were found with the MP2 densities.

It is known that geometries calculated at the MP2/6-31G* level usually agree quite well with experimental geometries. A comparison for the compounds in this study are shown in Table XI. The experimental geometries are usually averages at the zero-point vibrational level and are longer that the equilibrium geometry due to the anharmonicity of stretching vibrations. The bond lengths

calculated using MP2 are usually too long because it exaggerates the loss of charge density in the bonding region. Thus, the success of MP2 appears to be due at least in part to a cancellation of errors.

Acknowledgment. This investigation was supported by a grant from the National Science Foundation and by Lorentzian, Inc. C.M.H. gratefully acknowledges the Fannie and John Hertz Foundation for a predoctoral fellowship.

Band Structures and Molecular Properties of Polymers from Finite Cluster Calculations with Cyclic Periodic Boundary Conditions

Jayaraman Chandrasekhar*,† and Puspendu Kumar Das*,‡

Department of Organic Chemistry and Department of Inorganic and Physical Chemistry, Indian Institute of Science, Bangalore 560 012, India (Received: December 18, 1990)

The use of a finite cluster model with cyclic periodic boundary conditions for studying molecular and electronic structures of polymers within the MNDO framework is critically examined. A simple procedure is proposed to determine the k values corresponding to each of the discrete orbital energies obtained from the calculations. Thus, band structures can be effectively obtained from finite cluster models. The rapid convergence of the computed results with respect to the number and size of clusters chosen is demonstrated on the basis of the geometries, heats of formation per monomer, and orbital energies at common **k** points for *trans*-polyacetylene (PA). The band structures computed for polyacetylene (PA), poly(*p*-phenylene) (PPP), and polyacene (PAC) are generally within 0.1 eV of those obtained from detailed band calculations and show no edge effects. Preferred geometries, energies, ionization potentials, band structures, and band gaps have also been computed for polymethinimine (PMI) and polycyclobutadiene (PCBD). In agreement with experiment and/or other calculations, the present method correctly reproduces the Peierls distortion in PA and PMI and the preference for the "benzenoid" structure of PPP, but PCBD and PAC are found to have moderate band gaps.

Introduction

The power of computational methods for studying molecular and electronic structures of small molecules in the gas phase is now widely recognized. Several carefully parameterized semiempirical methods as well as ab initio procedures are routinely used to obtain new insights concerning structure, reactivity, and molecular properties, especially in organic systems.[1,2] However, corresponding applications in polymeric systems have been relatively sparse. The principal difficulty is in handling the large molecular size in such cases. Two extreme approaches have been made earlier to study infinite systems. A finite cluster, chosen as large as possible and terminated by inert groups like a hydrogen atom or an alkyl group, is assumed to be representative of the infinite chain.[3] While this procedure is computationally tolerable, important long-range effects may not be adequately described. Further, spurious edge effects may result due to the arbitrary termination of the infinite system. Occasionally, the results also vary with the way in which the oligomer is terminated, for example, in systems with quasi-degenerate ground states. The most serious flaw is that only discrete energy levels are obtained instead of smooth energy bands.

A more rigorous approach is to carry out a full band structure calculation, taking into account the translational symmetry present in the infinite systems by introducing the reciprocal **k** space. Thus, the calculation involves solving for a set of **k** vector dependent eigenvalues,[4] instead of one large matrix problem as in the finite cluster method. This procedure has been implemented within semiempirical as well as ab initio schemes, with applications focused on conducting organic polymers.[5]

Recently, Cui et al.[6] proposed an interesting simplified procedure to derive polymer properties from MNDO calculations on oligomers. To obtain band structures, an analogy based on Huckel results on finite and infinite systems was drawn. The discrete orbital energies obtained from finite cluster calculations were shown to correspond to specific **k** vector points of the polymer. Reliable energies were computed using a finite difference approach. Geometric parameters of the polymers were derived by exclusively considering the central portion of the oligomer, where the edge effects are less. While the above compound methodology has several attractive features, a number of deficiencies resulting from the termination of the oligomer chains remain, as pointed out by the authors themselves.[6] In this paper, we improve on their method by introducing periodic boundary conditions (PBC). The advantages of the procedure are demonstrated within the MNDO model for a number of one-dimensional polymers. The preferred geometries, heats of formation, and the band structures have been computed for different conformers of polyacetylene (PA), poly(*p*-phenylene) (PPP), and polyacene (PAC) for which detailed experimental and theoretical results are available. We have also examined polymethinimine (PMI) and polycyclobutadiene (PCBD) in view of current interest in designing conducting polymers through heteroatom perturbation and by using non-Kekule monomeric units.

Methodology

Within the Huckel MO model, analytic solutions are available for the orbital energies of a linear chain as well as a ring containing equivalent interacting orbitals. For a polyene chain of length M, the energies are given by

$$E_j(\text{linear}) = \alpha + 2\beta \cos(\pi j/(M+1)) \quad (1)$$

and, for a ring of N orbitals, by

$$E_j(\text{ring}) = \alpha + 2\beta \cos(2\pi j/N) \quad (2)$$

† Department of Organic Chemistry.
‡ Department of Inorganic and Physical Chemistry.

(1) Hehre, W. J.; Radom, L.; Pople, J. A.; Schleyer, P. v. R. *Ab Initio Molecular Orbital Theory*; Wiley: New York, 1986.
(2) Clark, T. *A Handbook of Computational Chemistry*; Wiley: New York, 1985.
(3) For typical recent studies, see: Barone, V. *Surf. Sci.* **1987**, *189/190*, 106. Russo, N.; Toscano, M. *J. Mol. Struct.* **1989**, *201*, 149.
(4) Kertesz, M. *Adv. Quantum Chem.* **1982**, *15*, 161. Seel, M. *Int. J. Quantum Chem.* **1984**, *26*, 753. Deak, P.; Snyder, L. *Int. J. Quantum Chem., Quantum Chem. Symp.* **1987**, *21*, 547.
(5) Dewar, M. J. S.; Yamaguchi, Y.; Suck, S. H. *Chem. Phys.* **1979**, *43*, 145. Kertesz, M.; Lee, Y. S. *J. Phys. Chem.* **1987**, *91*, 2690. Lee, Y. S.; Kertesz, M. *J. Chem. Phys.* **1988**, *88*, 2609. Hong, S. Y.; Kertesz, M. *Phys. Rev. Lett.* **1990**, *64*, 3031.
(6) Cui, C. X.; Kertesz, M.; Jiang, Y. *J. Phys. Chem.* **1990**, *94*, 5172.

0022-3654/92/2096-679$03.00/0